The interaction of infrared radiation with isolated molecules: intramolecular nonequilibrium

Eric Mazur, Kuei-Hsien Chen and Jyhpyng Wang

Department of Physics and Division of Applied Sciences, Harvard University, Cambridge, MA 01238

Anti-Stokes signals from various modes of isolated, infrared multiple photon excited molecules are measured to determine the intramolecular distribution of vibrational energy. This paper presents results for CF_2HCl, CF_2Cl_2, SF_6 and *1,1*-$C_2H_4F_2$. All but CF_2HCl exhibit collisionless changes in Raman spectrum after infrared multiphoton excitation. This shows that the excitation modifies the population of these modes. Even though the symmetric SF_6 molecule reaches an intramolecular equilibrium within the 20 ns time resolution of the experiment, the other molecules exhibit a distinct nonequilibrium intramolecular distribution of vibrational excitation energy.

Introduction

The rather surprising discovery, that isolated polyatomic molecules in the ground electronic state can absorb a large number of photons from a resonant high-power infrared laser,[1] has led to extensive experimental and theoretical studies of this phenomenon during the last decade.[2] Since the vibrational modes of a molecule are generally anharmonic,[3] one would expect the molecules to become out of resonance with an initially resonant laser field after the absorption of one or two photons (see Fig. 1a). The number of photons absorbed per molecule, however, can be as large as 30, and the increase in internal energy comparable to electronic excitation energies. Often the excitation results in collisionless dissociation of the molecules. Experiments showed that the absorption is a stepwise process and not a simultaneous absorption of many photons. The list of molecules that exhibit this behavior grows continuously,[4] and infrared multiphoton excitation evidently is a general property of all but the smallest polyatomic molecules.

Clearly, stepwise absorption of infrared laser photons up a single anharmonic vibrational manifold is not possible. This precludes the infrared multiple photon excitation of diatomic molecules. For a polyatomic molecule, consisting of N atoms, however, 3N–6 coupled anharmonic vibrational modes can participate in the process. In short the excitation mechanism can be explained as follows. At a certain level of excitation the density of states becomes very large and many quasi-isoenergetic (combinations of) states exist. In this high density of states region molecular excitation occurs through incoherent one-photon transitions. The high density of states and the anharmonic coupling of molecular modes provide a way for the molecules to continue to absorb photons. Fig. 1b schematically shows the absorption of one photon in this regime: a resonant mode absorbs a photon, and immediately 'dissipates' the energy to an intramolecular heat-bath formed by other nonresonant modes of the molecule.

Immediately the question arises how the absorbed energy is distributed among the various modes during this process. Do all modes participate, or are some excluded from the process? This question has received much attention because the excitation of only a few modes inside a molecule might lead to interesting new techniques for controlling chemical reactions. The large, and often not even known, number of states renders the problem inherently complicated from a theoretical point of view. Several authors have

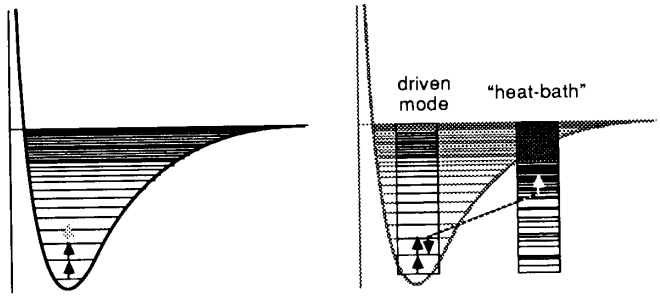

Fig. 1. Infrared excitation in a diatomic molecule (a) and multiple photon excitation in a polyatomic molecule (b). The diatomic molecule becomes out of resonance with the laser field after the absorption of one or two photons, even for very intense pulses when considerable power broadening occurs. Polyatomic molecules, however, have many vibrational modes which are coupled by cross-anharmonicities. Multiple photon excitation can then take place through stepwise incoherent excitation between combinations of states. Because other modes participate in the process, energy slowly 'leaks' into these modes. The figure shows one possible intramolecular energy exchange.

proposed a statistical description of the ensemble of modes,[5,6] suggesting an intramolecular equilibrium distribution of vibrational energy among the various modes of an isolated infrared multiphoton excited molecule.

Direct information on the intramolecular energy distribution in highly excited molecules was obtained experimentally with pump-probe type experiments, such as infrared double resonance experiments[7–9] and spontaneous[10–17] and coherent[18,19] Raman experiments. Raman spectroscopy was first employed by Bagratashvili and coworkers[10] and later by our group[16] as a tool for studying infrared multiple photon excitation. Fig. 2 schematically shows the general concept of these experiments. First, an intense infrared laser pulse, resonant with a particular infrared active mode (shown at the right), excites an isolated molecule. The figure shows one possible excitation pathway: after the (coherent) absorption of a few photons at the bottom of the resonant vibrational ladder, the molecule reaches the high density of states region known as the quasicontinuum (shown in the figure as an overlap of the various modes), and energy starts to 'leak' to other modes. After the excitation a second laser pulse probes one Raman-active mode from the intramolecular 'heat-bath' of modes (shown at the left). At room temperature the population of excited states of the Raman active modes is only a few percent, so that without infrared excitation only a Stokes signal is observed (Fig. 2, transition 1). If some high lying states of the Raman active mode participate in the excitation process they may become populated. Because of the anharmonicity of the Raman active mode, a shift in Stokes signal is then observed[13] (Fig. 2, transition 2), and an anti-Stokes signal appears (Fig. 2, transition 3). Anti-Stokes scattering is a particularly sensitive probe for the population of excited levels in the Raman active mode, because of the absence of signal without excitation.

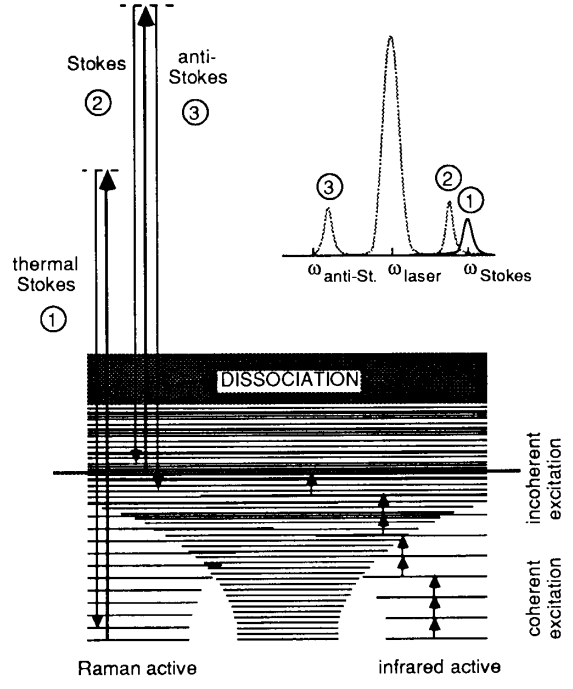

Fig. 2. Spontaneous Raman spectroscopy of infrared multiple photon excited molecules. After irradiation with an intense infrared pulse the molecules reach a region of high density of states known as the 'quasicontinuum'. Molecules that remain in the lower vibrational states (cold molecules) show only Stokes scattering (1), while the highly excited ones (hot molecules) show both a shifted Stokes (2) and an anti-Stokes signal (3).

In simple harmonic approximation one can readily show that the transition probabilities $W_{n\to n+1}$ and $W_{n\to n-1}$, for Stokes and anti-Stokes transition respectively, are proportional to the quantum number n.[17] Therefore the intensity of the Stokes and anti-Stokes signals are proportional to the average total energy in the mode, $E_R = h\nu_R \Sigma\, n\, N(n)$, with ν_R the frequency of the Raman active mode, and $N(n)$ the population of level n.

$$I_S \sim \sum_{n=0}^{\infty} W_{n\to n+1} N(n) \sim \sum_{n=0}^{\infty} (n+1) N(n) = \frac{E_R}{h\nu_R} + 1, \quad (1)$$

$$I_{AS} \sim \sum_{n=0}^{\infty} W_{n\to n-1} N(n) \sim \sum_{n=0}^{\infty} n\, N(n) = \frac{E_R}{h\nu_R}. \quad (2)$$

From these equations it follows that if the infrared multiphoton excitation alters the population of the levels in the Raman active mode, the Stokes and anti-Stokes signal intensities will change. Thus, spontaneous Raman spectroscopy allows one to determine experimentally the role of various modes in the infrared multiple photon excitation process.

Experimental setup

The experimental setup, shown schematically in Fig. 3, is discussed in detail in a previous paper.[16,17] Basically, molecules excited by a pulse of either 0.5 or 15 ns duration from a high power tunable CO_2-laser are probed by frequency-doubled ruby laser pulse of 20 ns duration. The two laser beams cross in a low pressure cell and scattered light from the interaction region is detected in a direction perpendicular to the two beams. A low resolution monochromator (1-2 nm) separates the Raman light from elastically scattered light. Spectral resolution is sacrificed for nanosecond time resolution and signal intensity (to enable measurement at low density).[20] For each pulse the infrared pulse energy and the time delay between the pump and the probe pulse is measured.

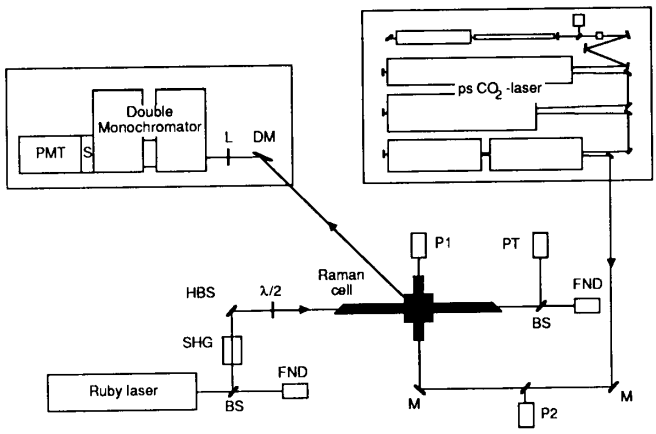

Fig. 3. Setup for the measurement of spontaneous Raman scattering from infrared multiphoton excited molecules at low densities. BS = beam splitter, SHG = second harmonic generator, HBS = harmonic beam splitter, $\lambda/2$ = half-wave plate, FND = fast photodiode, PT = phototube, P1, P2 = pyroelectric detector, M = mirror, DM = dichroic mirror, L = quartz lens, S = shutter, PMT = photomultiplier tube.

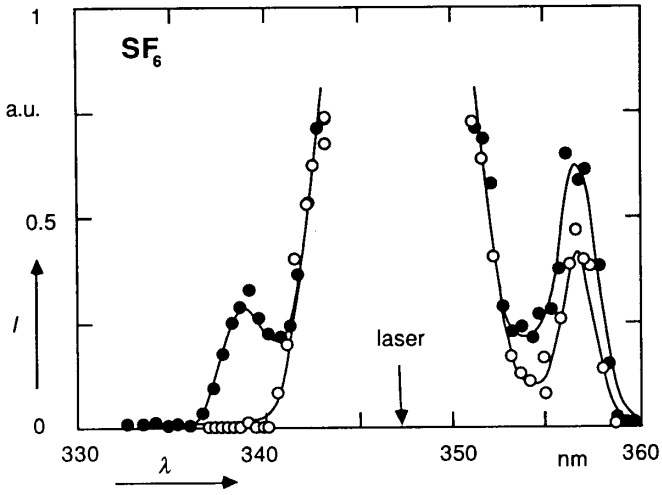

Fig. 4. Raman spectrum of SF_6, with (closed symbols) and without (open symbols) infrared multiphoton excitation. Infrared excitation: 10.6 μm P(20) line, 0.5 ns (squares) and 15 ns (circles) pulse duration, both at an average fluence of 0.6×10^4 J/m^2. The small arrow shows the position of the laser radiation at 347.15 nm.

To isolate intramolecular from (collisional) intermolecular effects the signals are measured at pressures low enough to ensure that no significant collisional relaxation of vibrational energy occurs on the time scale of the experiment. Since the gas-kinetic mean-free time τ_{mf} is roughly given by $p\tau_{mf} \approx 10^4$ ns Pa, and the probe pulse limits the time resolution of the experiment to 20 ns, one has to work at pressures of 400 Pa (3 torr) or lower. The Raman signals then correspond to single photon counts, and therefore the data must be averaged over at least 10^4 pulses to obtain a satisfactory signal-to-noise ratio. At the end of a measurement the data points are sorted out according to infrared pump intensity and time-delay between pump and probe, and averaged.

Experimental results and discussion

Four different molecules, CF_2HCl, CF_2Cl_2, SF_6 and *1,1*–$C_2H_4F_2$, varying in size from five to eight atoms, were studied with the present apparatus. Figs. 3 through 9 show some of the experimental results. Table I presents some relevant molecular data as well as an overview of the experimental results. All measurements were carried out at room temperature, with gas pressures ranging from 14 to 500 Pa and with infrared fluences up to 8×10^4 J/m^2. The commercially obtained gases have a reported purity better than 99.9%.

1. *SF_6*: Measurements on this symmetric molecule have been reported in detail previously.[17] This molecule has only one accessible Raman active mode, ν_1, with a Raman shift of 775 cm^{-1}. Data were obtained for CO_2-laser frequencies between the P(12) and the P(28) lines of the 10.6 μm branch, which are resonant with the triply degenerate infrared active ν_3-mode (944 cm^{-1}). Two different pulse durations were employed: 0.5 and 15 ns full-width at half-maximum pulses.

Fig. 4 shows the (low resolution) Raman spectrum with and without infrared pumping. As expected, the molecules show only a Stokes signal at room temperature. After excitation, however, an anti-Stokes signal appears, and at the same time the Stokes signal increases in accordance with Eqs. (1) and (2). These changes occur on time scales several orders of magnitude shorter than the average time between collisions.

Fig. 5 shows the increase in Stokes and anti-Stokes signals, measured at 356.7 and 338 nm respectively, as a function of the time delay between the pump and the probe pulse for two infrared pulse durations. The signals for negative time delay ($t < 0$, room temperature equilibrium) serve as calibration for the Raman signals. At $t = 0$ infrared excitation takes place and the Raman signals increase. Within the experimental accuracy both Stokes and anti-Stokes signal increase by the same amount, in accordance with Eqs. (1) and (2). The rise time of the signals is determined by the 20 ns pulse duration of the second harmonic of the probe laser. However, even though not resolved in these measurements, the increase in signal

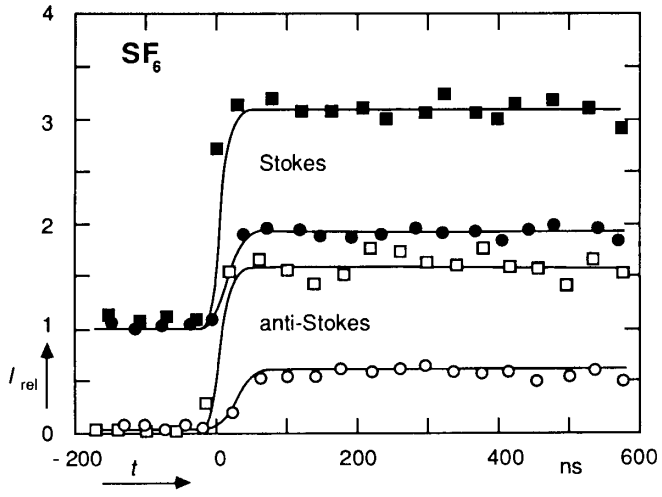

Fig. 5. Intensity of Stokes (closed symbols) and anti-Stokes (open symbols) signals of SF_6 as a function of the time delay between pump and probe pulses at a pressure of 67 Pa. The data are normalized to the thermal Stokes signal. Negative time delay means that the signals are measured before the infrared multiphoton excitation. The rise time in the curves reflects the 20 ns FWHM duration of the probe pulse. These results were obtained for 0.5 ns infrared excitation at the 10.6 μm P(20) line, with an average fluence of 0.8×10^4 J/m^2.

clearly occurs on a time-scale much shorter than the mean free time between collisions (about 200 ns at a pressure of 67 Pa). The pressure dependence of the signals, which is not presented here, shows that the increase in signal is not due to collisions, but is truly a *collisionless* phenomenon.[17] Interestingly enough the signals remain constant, even on a time scale on which collisional vibrational energy relaxation occurs.[21] For longer delay times ($t > 2$ μs), diffusion of the excited molecules out of the probing region causes the signals to revert to their original values.[17]

The dependence of the anti-Stokes signal intensity on the infrared laser fluence (energy per unit area) is shown in Fig. 6 for different pressures and pulse durations. These results were obtained in separate experimental runs, as indicated by the different symbols. The data obtained for the two pulse durations show that at low fluence the signals depend on the exciting laser pulse intensity: a larger increase in Raman signal occurs at the shorter, higher intensity, pulses. At low excitation one needs a high intensity for *coherent* multiphoton excitation through the lower part of the vibrational ladder. At the higher fluences, once the molecules are highly excited, the curves for the 0.5 and 15 ns pulse durations approach each other, and the dependence of the signal intensity on laser pulse intensity vanishes. This is consistent with the concept of a quasicontinuum[5] at high excitation, and agrees with the behavior observed in photoacoustic measurements, which determine the total amount of energy absorbed per molecule.[22]

The main purpose of this research is to obtain information on the role of nonresonant modes in the multiphoton excitation of polyatomic molecules. The observed collisionless changes in Raman signals provide clear and direct evidence that some of the nonresonant modes do indeed participate in the excitation process. Since the intensity of the signals is proportional to the average energy in the mode, one can determine E_R from the ratio of the anti-Stokes intensity to the thermal room temperature value of the Stokes signal, I_S^0. From Eqs. (1) and (2), one obtains

Table I. Overview of molecular data and experimental results.

Molecule	Number of atoms	Symmetric	Pump mode (cm^{-1})	CO_2-line (cm^{-1})	Raman lines (cm^{-1})	Equilibrium
CF_2HCl	5	no	1108	9.4 μm R(32); 1086	587,[2] 800,[2] 1134,[2] 1325,[2] 3029 [2]	no?
CF_2Cl_2	5	no	919	10.6 μm P(32); 933	664,[1] 919,[1] 1082,[1] 1147[3]	no
SF_6	7	yes	944	10.6 μm P(20); 944	775 [1]	yes
$C_2H_4F_2$	8	no	942	10.6 μm P(20); 944	870 [1], 1141,[2] 1457,[2] 2978[2]	no

[1] Measured in this experiment: exhibits change in intensity after infrared excitation
[2] Measured in this experiment: no measurable change in intensity
[3] Not measured; very weak

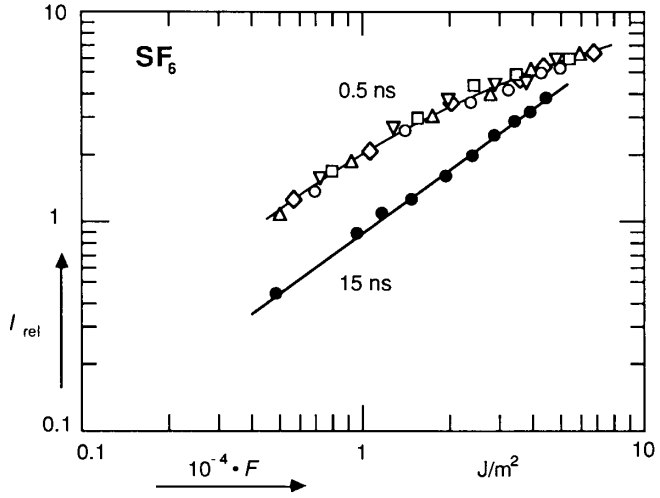

Fig. 6. Fluence dependence of anti-Stokes signal for SF_6. Relative anti-Stokes signal as a function of the infrared pump fluence for various pressures and two infrared pulse durations, at the 10.6 μm P(20) line: 0.5 ns (open symbols) and 15 ns (closed symbols). This graph shows the reproducibility of the data from measurement to measurement.
□: 33 Pa; ○: 67 Pa; △: 133 Pa; ▽: 200 Pa; ◇: 267 Pa; ●: 133 Pa.

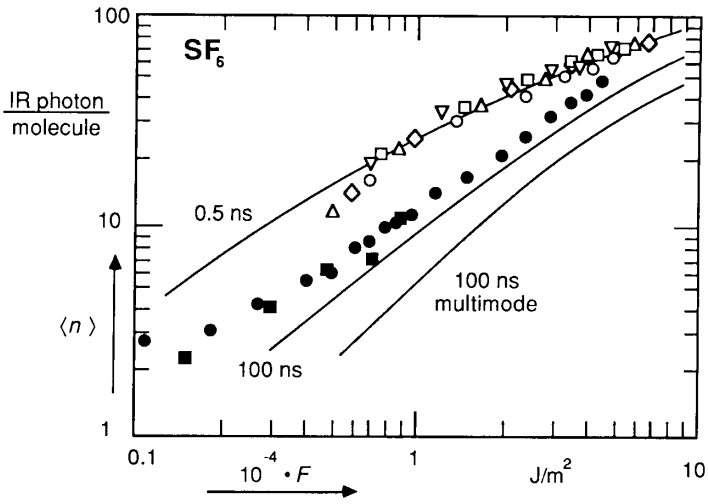

Fig. 7. Comparison with photoacoustic measurements for SF_6. The average number of infrared photons absorbed per molecule is plotted as a function of infrared fluence. The data points shown were obtained from the ones shown in Fig. 6, assuming thermal equilibrium between all vibrational modes immediately after the infrared multiphoton excitation. The solid lines show the average number of infrared photons obtained from photoacoustic measurements. The results show a remarkable agreement.

$$I_{rel} \equiv \frac{I_{AS}}{I_S^o} = \frac{E_R}{h\nu_R + E_R^o}, \qquad (3)$$

with E_R^o the room temperature equilibrium value of E_R.

Unfortunately the lack of more than one accessible Raman active mode for SF_6 makes it impossible to compare the energy in different modes. This limits us therefore to a comparison of E_R with the average total energy absorbed per molecule, $\langle E \rangle$, known from photoacoustic measurements. One may also write

$$\langle E \rangle = \langle n \rangle h\nu_R, \qquad (4)$$

with $\langle n \rangle$ the average number of infrared photons absorbed per molecule. If the intramolecular distribution of energy has reached equilibrium, $\langle E \rangle$ may be obtained from E_R and compared to the value of $\langle n \rangle$ determined in photoacoustic measurements. This is done in Fig. 7, which shows $\langle n \rangle$ as a function of fluence. The data points correspond to the data points in Fig. 6 (assuming intramolecular equilibrium), and the curves show the results obtained from photoacoustic measurement. The data agree remarkably well, suggesting that for SF_6 the intramolecular energy distribution indeed equilibrates. The absence of a decay of the Raman signals in Fig. 4 further supports this suggestion. Even though the initially nonequilibrium *intermolecular* distribution of energy equilibrates,[13] E_R remains constant once intramolecular equilibrium is achieved. In the absence of intramolecular equilibrium, one would expect E_R, and consequently the signal intensities, to change on a much shorter time scale because of a rearrangement of energy over the various vibrational modes.

2. *CF_2HCl*: This molecule has five accessible Raman active modes of widely different energy (600—3000 cm^{-1}). The peak absorption of this molecule coincides with the 9.4 μm R(32) CO_2 laser line at 1086 cm^{-1}. Even at the maximum fluence at this line (2×10^4 J/m^2), none of the five Raman lines show any detectable change in intensity. Photoacoustic studies[23] of the infrared multiphoton excitation of this molecule have shown that at such a fluence the molecules absorb about ten infrared photons. The absence of anti-Stokes scattering from low lying levels, such as the Raman active mode at 587 cm^{-1}, suggests that not all modes participate in the excitation process. This leads to the conclusion that the energy distribution for this molecule does not equilibrate without collisions.

3. *1,1–$C_2H_4F_2$*: This asymmetric isomer has four accessible Raman modes. Data were obtained for 0.5 ns long pulses at the P(20) line of the 10.6 μm branch, which is resonant with the infrared active C—F stretch mode at 942 cm^{-1}. At fluences above 1.5×10^4 J/m^2, an intense broadband fluorescence appears. At those fluences the molecules apparently dissociate, and the probe laser induces a

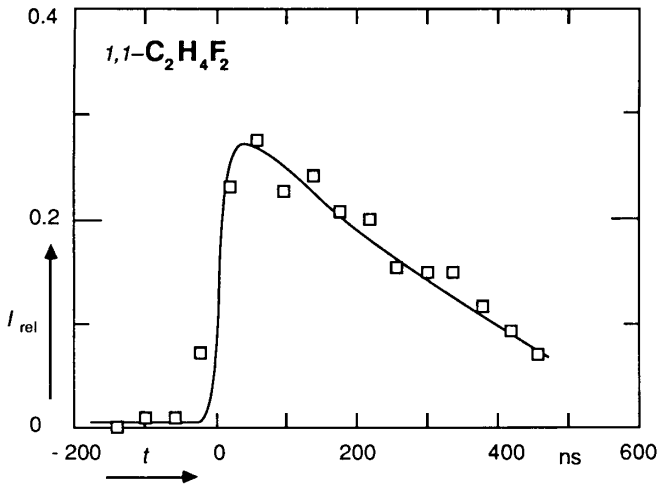

Fig. 8. Intensity of anti-Stokes signal for the 870 cm^{-1} mode of *1,1*–$C_2H_4F_2$ as a function of the time delay between pump and probe pulses at a pressure of 660 Pa. The data show a behavior distinctly different from the one for SF_6. These results were obtained for 0.5 ns infrared excitation at the 10.6 μm P(20) line, with an average fluence of 1.5×10^4 J/m^2.

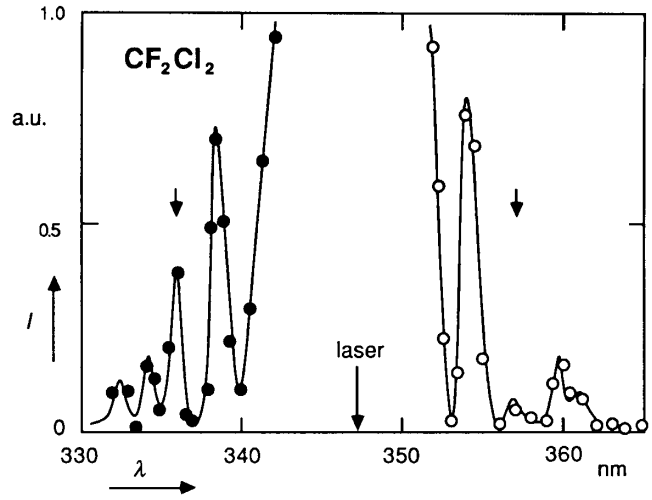

Fig. 9. Stokes spectrum of CF_2Cl_2 without infrared multiple photon excitation (open symbols) and anti-Stokes spectrum with infrared multiphoton excitation (closed symbols). Infrared excitation: 10.6 μm P(32) line, and 15 ns pulse duration. The arrows mark the positions of the laser radiation at 347.15 nm, and the pumped mode at 919 cm^{-1}. The ratio of anti-Stokes to (corresponding) Stokes peak intensities clearly show that the pump mode is the 'hottest' mode after the infrared multiphoton excitation.

fluorescence from the dissociation fragments. This laser induced fluorescence extends far (at least 3000 cm^{-1}) into the anti-Stokes side of the spectrum, which indicates that the dissociation fragments carry a considerable amount of excitation energy. One can discriminate the fluorescence from Raman scattering either spectrally or temporally. The fluorescence has a broad continuous spectrum and a long decay (μs), while the spectrally discrete Raman signals (see Figs. 4 and 9) coincide with the 20 ns probe pulse. Since the present measurements are carried out at fixed wavelengths, only temporal discrimination can be applied. A fast electronic circuit therefore monitors the coincidence of the signals with the probe pulse, and flags the data point if any signal appears after the probe.[24] The analysis is then limited to either fluorescence or Raman signals. We restrict ourselves here to a discussion of the Raman signals. Up to the dissociation threshold, only one of the Raman active lines, at 870 cm^{-1}, shows a small but measurable amount of anti-Stokes signal after excitation.

Fig. 8 shows the time-dependence of the anti-Stokes signal for the mode at 870 cm^{-1} at a pressure of 660 Pa and a fluence of 1.5×10^4 J/m^2. Again a short collisionless increase in signal occurs. In contrast to SF_6, however, the anti-Stokes signal shows a decay on a time scale of the same order of magnitude as collisional vibrational relaxation. This, combined with the fact that no other Raman active mode exhibits any change up to the dissociation of the molecule, indicates that for this particular molecule too, the vibrational energy does not reach equilibrium.

The pumped C—F stretch of *1,1*–$C_2H_4F_2$ is a highly asymmetric vibrational mode. It is consequently not surprising that almost no coupling to the (symmetric) Raman active modes takes place. Measurements on the other isomer, *1,2*–$C_2H_4F_2$, with a much more symmetric C—F stretch, might therefore lead to a better insight of the role of symmetry in the coupling of vibrational modes.

4. *CF_2Cl_2*: This five atom molecule has four accessible Raman active modes, three of which, at a shift of 664, 919, and 1082 cm^{-1} respectively, were measured after infrared multiphoton excitation. The C—Cl stretch mode at 919 cm^{-1} is both infrared and Raman active and can be pumped with the P(32) line of the 10.6 μm branch of the CO_2 laser. This allows to directly observe the energy in the pump mode and compare it with the energy in other modes. The measurements presented here were all carried out at a gas pressure of 400 Pa. For this molecule too, broadband laser induced fluorescence appears at fluences above 1.8×10^4 J/m^2.[25]

Fig. 9 shows the Raman spectrum of CF_2Cl_2 with and without infrared multiphoton excitation. At 400 Pa and room temperature, the equilibrium anti-Stokes signal cannot be detected because of the small population of excited levels. The anti-Stokes part of the spectrum therefore shows the increase in energy in the four vibrational modes. The pump mode, indicated in the graph with small arrows, clearly contains the largest amount of energy (see the anti-Stokes—Stokes intensity ratio). Surprisingly enough, the mode at 664 cm^{-1} remains relatively 'cold'. Changes in

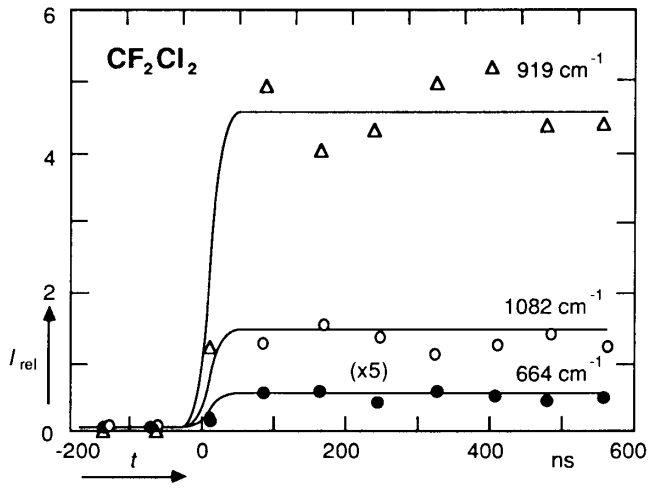

Fig. 10. Intensity of normalized anti-Stokes signals for three modes of CF_2Cl_2 as a function of the time delay between pump and probe pulses at a pressure of 400 Pa. The data points for the mode at 664 cm^{-1} are multiplied by 5. These results were obtained for 15 ns infrared excitation at the 10.6 μm P(32) line, with an average fluence of 1×10^4 J/m^2.

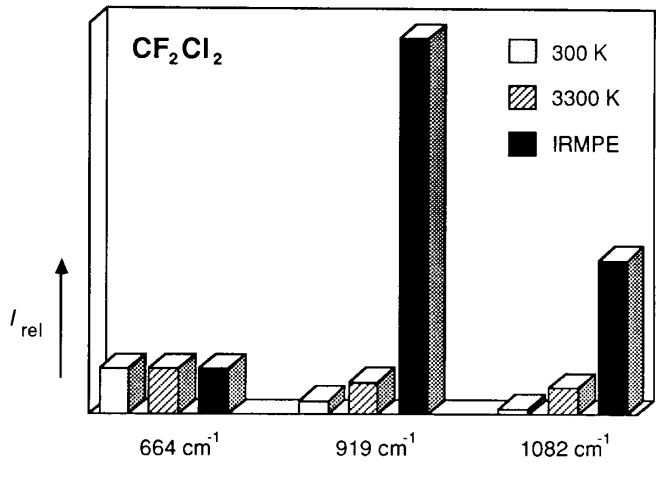

Fig. 11. Comparison of the anti-Stokes to Stokes intensity ratios for 3 modes of CF_2Cl_2. The grey bars are calculated from the equilibrium intensities at 300 K and 3300 K. The black bars show ratios obtained after infrared multiple photon excitation. For clarity the intensities for 300 K and 3300 K have been multiplied by 6.2 and 0.1, respectively.

energy of modes with a larger energy step than the energy of the infrared photons (1082 and 1147 *vs.* 933 cm^{-1}) also occur.

In Fig. 10 the anti-Stokes signals of three modes, normalized with the corresponding room temperature Stokes signal, are plotted as a function of time. Again the signals rise in 20 ns and remain constant up to 600 ns. We can now assess the distribution of energy over these three modes. From the ratio of anti-Stokes to room temperature Stokes signal in Figs. 9 and 10 one can immediately deduce that the distribution has not reached equilibrium. Fig. 11 compares these ratios for the three modes in equilibrium at both 300 K and 3300 K with the ratio obtained in the present experiment. A temperature of 3300 K equals an increase in internal vibrational energy corresponding to 19 infrared laser photons. The graph clearly shows that the intramolecular distribution of energy of CF_2Cl_2 is not in equilibrium, and that the pump mode is much more highly excited than the other Raman active modes.

Conclusion

This paper presents the results of measurements of various collisionless infrared multiphoton excited molecules. The amount of energy in various modes of these molecules is determined from the spontaneous Raman scattering of each of these modes. After infrared multiphoton excitation a collisionless change in energy distribution takes place within the 20 ns time resolution. Whereas the distribution of vibrational energy over the different modes is in equilibrium for the symmetric SF_6, the other (not symmetric) molecules show a distinct nonequilibrium distribution.

Acknowledgments

The research for this paper is supported by the Army Research Office and the Joint Services Electronics Program under contracts with Harvard University.[26]

1 N.R. Isenor, V. Merchant, R.S. Hallsworth and M.C. Richardson, Can. J. Phys. 51, 1281 (1973).

2 See e.g. the following publications and references therein: V.N. Bagratashvili, V.S. Letokhov, A.A. Makarov, E.A. Ryabov, Multiple Photon Infrared Laser Photophysics and Photochemistry (Harwood Academic Publishers, New York, 1985); N. Bloembergen and E. Yablonovitch, Physics Today 5, 23 (1978) W. Fuss and K. L. Kompa, Prog. Quant. Electr. 7, 117 (1981); D.S. King, Dynamics of the Excited State, Ed. K. P. Lawley (Wiley, New York, 1982).

3 G. Herzberg, Molecular spectra and molecular structure, Vol. 2 (Van Nostrand Reinhold, New York, 1979).

[4] See almost any issue of J. Chem. Phys.
[5] N. Bloembergen and E. Yablonovitch, Physics Today 5, 23 (1978).
[6] H.W. Galbraith and J.R. Ackerhalt, in Laser induced Chemical Processes, Ed. J.I. Steinfeld (Plenum, New York, 1981).
[7] D.S. Frankel and T.J. Manuccia, Chem. Phys. Lett. 54, 451 (1978).
[8] R.C. Sharp, E. Yablonovitch and N. Bloembergen, J. Chem. Phys. 74, 5357 (1981).
[9] P. Mukherjee and H.S. Kwok, J. Chem. Phys. 84, 1285 (1986).
[10] V.N. Bagratashvili, Yu.G. Vainer, V.S. Doljikov, S.F. Koliakov, A.A. Makarov, L.P. Malyavkin, E.A. Ryabov, E.G. Silkis, and V.D. Titov, Appl. Phys. 22, 101 (1980).
[11] V.N. Bagratashvili, Yu.G. Vainer, V.S. Dolzhikov, S.F. Kol'yakov, V.S. Letokhov, A.A. Makarov, L.P. Malyavkin, E.A. Ryabov, E.G. Sil'kis, and V.D. Titov, Sov. Phys. JETP 53, 512 (1981).
[12] V.N. Bagratashvili, V.S. Doljikov, V.S. Letokhov, A.A. Makarov, L.P. Maljavkin, E.A. Ryabov, E.G. Silkis, and Yu.G. Vainer, Opt. Comm. 38, 31 (1981).
[13] V.N. Bagratashvili, Yu.G. Vainer, V.S. Doljikov, V.S. Letokhov, A.A. Makarov, L.P. Malyavkin, E.A. Ryabov, and E.G. Sil'kis, Opt. Lett. 6, 148 (1981).
[14] Yu.S. Doljikov, V.S. Letokhov, A.A. Makarov, A.L. Malinovsky and E.A. Ryabov, Chem. Phys. Lett. 124, 304 (1986).
[15] V.S. Doljikov, Yu.S. Doljikov, V.S. Letokhov, A.A. Makarov, A.L. Malinovsky and E.A. Ryabov, Chem. Phys. 102, 155 (1986).
[16] E. Mazur, I. Burak, and N. Bloembergen, Chem. Phys. Lett. 105, 258 (1984).
[17] Jyhpyng Wang, Kuei-Hsien Chen and Eric Mazur, Phys. Rev. A **34**, 3892 (1986).
[18] R.V. Ambartsumyan, S.A. Akhmanov, A.M. Brodnikovskii, S.M. Gladkov, A.V. Evseev, V.N. Zadkov, M.G. Karimov, N.I. Koroteev, and A.A. Puretskii, JETP Lett. **35**, 210 (1982).
[19] S.S. Alimpiev, S.I. Valyanskii, S.M. Nikiforov, V.V. Smirnov, B.G. Sartakov, V.I. Fabelinskii, and A.L. Shtarkov, JETP Letters, **35**, 360 (1982).
[20] Eric Mazur, Rev. Sci. Instrum. **57**, 2507 (1986).
[21] R.D. Bates Jr., J.T. Knudtson, G.W. Flynn and A.M. Ronn, Chem. Phys. Lett. 8, 103 (1971)
[22] J.G. Black, P. Kolodner, M.J. Schultz, E. Yablonovitch, and N. Bloembergen, Phys. Rev. A **19**, 704 (1979).
[23] T.B. Simpson, J.G. Black, I. Burak, E. Yablonovitch and N. Bloembergen, J. Chem. Phys. 83, 628 (1985)
[24] Jyhpyng Wang and Eric Mazur, Rev. Sci. Instrum. to be published.
[25] Kuei-Hsien Chen, Jyhpyng Wang and Eric Mazur, to be published.
[26] Contract numbers: DAAG29-85-K-0600 and N00014-84-K-0465 , respectively.